Published in final edited form as:
Virology. 2011 January 20; 409(2): 262–270. doi:10.1016/j.virol.2010.10.016.

The Flv^r-encoded murine oligoadenylate synthetase 1b (Oas1b) suppresses 2-5A synthesis in intact cells

H. Elbahesh[1], **B. K. Jha**[2], **R. H. Silverman**[2], **S. V. Scherbik**[1], and **M. A. Brinton**[1]

[1]Department of Biology, Georgia State University, Atlanta, GA

[2]Lerner Research Institute, Cleveland Clinic, Cleveland, OH, USA

Abstract

Resistance to flavivirus-induced disease in mice is conferred by the autosomal gene *Flv*, identified as 2′-5′ oligoadenylate synthetase 1b (Oas1b). Resistant mice express a full-length Oas1b protein while susceptible mice express the truncated Oas1btr. In this study, Oas1b was shown to be an inactive synthetase. Although the Oas/RNase L pathway was previously shown to have an antiviral role during flavivirus infections, Oas1b protein inhibited Oas1a *in vitro* synthetase activity in a dose-dependent manner and reduced 2-5A production *in vivo* in response to poly(I:C). These findings suggest that negative regulation of 2-5A by inactive Oas1 proteins may fine tune the RNase L response that if not tightly controlled could cause significant damage in cells. The results also indicate that flavivirus resistance conferred by Oas1b is not mediated by 2-5A. Instead, Oas1b inhibits flavivirus replication by an alternative mechanism that overrides the proviral effect of reducing 2-5A accumulation and RNase L activation.

Keywords

2′-5′ oligoadenylate synthetase; RNase L; 2-5A; flavivirus; RNA-protein interaction

Introduction

The genus *Flavivirus* includes a number of mosquito borne human pathogens, such as yellow fever virus, dengue virus, Japanese encephalitis virus, and West Nile virus (WNV). A number of factors such as the age, immune status and genetic makeup of the host as well as the route of inoculation, dose and virulence of the infecting virus can influence the outcome of flavivirus infections (Brinton, 2002). In mice, the alleles of an autosomal gene (*Flv*) determine resistance/susceptibility to flavivirus-induced disease. Mice carrying the resistant allele (*Flv*^{r}) are not resistant to flavivirus infection but produce significantly lower levels of virus compared to susceptible mice. The *Flv* gene was identified as 2′-5′ oligoadenylate synthetase 1b (Oas1b) (Mashimo et al., 2002; Perelygin et al., 2002). Resistant mice express a full-length Oas1b protein while susceptible mice express a truncated Oas1b protein (Oas1btr) generated by a premature stop-codon. The majority of inbred mouse strains used in laboratories are homozygous for the susceptibility allele (*Flv*^{s}).

***Corresponding author:** Margo A. Brinton, Ph.D. Department of Biology Georgia State University P.O. Box 4010 Atlanta, GA 30302-4010 Phone: (404) 413-5388; Fax: (404) 413-5301 mbrinton@gsu.edu .

In mice, the 2′-5′ olioadenylate synthetase family consists of eight small *Oas1* genes (*Oas1a* through *Oas1h)*, an *Oas2* gene, an *Oas3* gene, and two Oas-like genes (*OasL1* and *OasL2)* (Kakuta, Shibata, and Iwakura, 2002). The Oas1 proteins contain a single 2′-5′ oligoadenylate synthetase unit, while two and three copies are present in the Oas2 and Oas3 proteins, respectively. The OasL proteins contain a single OAS unit as well as two C-terminal ubiquitin-like domains (Hartmann et al., 1998b; Rebouillat, Marie, and Hovanessian, 1998). The members of the 2′-5′ oligoadenylate synthetase family are interferon-inducible genes (ISGs) and were previously reported to be upregulated in WNV infected cells (Scherbik, Stockman, and Brinton, 2007). 2′-5′ oligoadenylate synthetases are activated by binding to dsRNA and polymerize ATP into short 2′-5′ linked oligoadenylates (2-5A) (Kerr and Brown, 1978). The 2-5A binds to RNase L in the cytosol which leads to activation and dimerization of RNase L (Floyd-Smith, Slattery, and Lengyel, 1981). Activated RNase L cleaves viral and cellular single-stranded RNAs after UA and UU dinucleotides (Wreschner et al., 1981). Activated RNase L was previously reported to have an antiviral effect against WNV infections in mouse embryofibroblasts (MEFs) from both flavivirus-resistant and -susceptible mice (Scherbik et al., 2006). The virus-nonspecific nature of 2-5A production and RNase L-mediated RNA degradation are not consistent with the flavivirus-specific phenotype of the *Flv* gene suggesting that Oas1b mediates flavivirus-resistance through a novel mechanism unrelated to the 2-5A/RNase L pathway.

The N-terminal sequence of human OAS1 proteins contains an LXXXP motif previously shown to be required for synthetase activity (Ghosh et al., 1997a). The catalytic domain contains a nucleotidyltransferase fold, a P-loop motif, three catalytic aspartic acid residues, and the substrate acceptor binding site (Yamamoto, Sono, and Sokawa, 2000). The substrate donor binding site and a CFK motif are located in the C-terminal domain. The catalytic aspartic acid triad forms a Mg^{2+}-binding DAD motif. It has been suggested that the putative RNA activation site spans both the catalytic domain and C-terminal domain in the human OAS1 protein and contains a lysine/arginine rich motif (KR-rich motif). The P-loop, DAD catalytic triad, and KR-rich motif are required for the synthetase activity of most OASs (Saraste,Sibbald, and Wittinghofer, 1990; Yamamoto, Sono, and Sokawa, 2000). Although the CFK motif has been shown to be required for the synthetase activity of the human OAS proteins, this motif is not conserved within the active murine Oas1a and Oas1g proteins and is therefore unlikely to affect the structural stability of the murine proteins.

In the present study, Oas1b was shown to lack synthetase activity. This finding is consistent with previous data indicating that the flavivirus resistance phenotype mediated by Oas1b does not involve the 2-5A antiviral pathway (Scherbik et al., 2006). Full-length Oas1b, but not Oas1btr (the truncated protein encoded by Flv^s), was able to inhibit the *in vitro* synthetase activity of Oas1a in a dose-dependent manner and reduced poly(I:C)-stimulated 2-5A production *in vivo*. The results suggest that full-length Oas1b, but not the truncated protein Oas1b, functions as a dominant negative inhibitor of 2-5A oligonucleotide synthetase activity.

Results

Assay of the 2-5A synthetase activity of recombinant Oas1b proteins

In a previous study, unpurified lysates from bacteria expressing individual recombinant murine Oas1 proteins fused to an N-terminal 10X histidine tag were tested for 2-5A synthetase activity and poly(I:C) binding activity (Kakuta, Shibata, and Iwakura, 2002). Only Oas1a and Oas1g were shown to be active 2-5A synthetases but all eight of the Oas1 proteins (Oas1a through h) tested were able to bind poly(I:C). The Oas1 cDNAs used in that study were cloned from flavivirus-susceptible C57BL/6J mice and so Oas1btr but not Oas1b was analyzed.

To test the synthetase activity of the full-length Oas1b protein, recombinant Oas1b, Oas1a (positive control) and Oas1btr (negative control) proteins fused to an N-terminal 42.5 kDa maltose binding protein (MBP) were expressed in bacteria and partially purified on amylose resin columns. Fusion proteins of the expected molecular masses, Oas1a (~85 kD), Oas1b (~86 kDa) and Oas1btr (~71 kDa) were detected by Coomassie blue staining after separation of proteins by 10% SDS-PAGE (Fig. 1A). The average purity of Oas1a and Oas1btr was ~80% while that of Oas1b was ~60 to 75%. The identity of the recombinant proteins was confirmed by immunoblotting with anti-MBP (Fig. 1B) and anti-Oas antibody (Fig. 1 C). Some breakdown of the Oas1b protein was observed as indicated by the minor ~35 kDa band (N-terminal fragment) on the anti-MBP Western blot (Fig. 1B) and the ~55 kDa band (C-terminal fragment) on the anti-Oas Western blot (Fig. 1C).

To determine whether the MBP-tag negatively affected the enzymatic activity of Oas1a, the synthetase activity of the MBP-Oas1a fusion protein was compared to that of the Oas1a protein after removal of the tag with Genenase I (Fig 2A, lane 3). The proteins were incubated with poly(I:C) and α-^{32}pATP at 30°C for 18 hrs. The 2-5A produced were separated by denaturing 8M urea 20% PAGE and visualized by autoradiography. Dimer, trimer, tetramer and higher order products were produced by reactions containing MBP-Oas1a at concentrations ranging from 0.5 μg (117 nM) to 16 μg (3.76 μM) (Fig. 2A, lanes 4-7). The level of 2-5A synthesized by MBP-Oas1a was similar to that previously reported using a similar concentration of a His-tagged recombinant Oas1a protein under similar reaction conditions (Kakuta, Shibata, and Iwakura, 2002;Yan et al., 2005). The cleaved and fused Oas1a proteins produced similar levels of 2-5A, indicating that the MBP tag did not negatively affect Oas1a synthetase activity (Fig. 2A, lanes 3 and 4). As expected, synthetase activity was not detected in the reaction containing MBP (Fig. 2A, lane 2). Neither MBP-Oas1b nor MBP-Oas1btr produced detectable 2-5A when added to the reactions at concentrations of 2.6 μg (638 nM) or 2.3 μg (605 nM), respectively (Fig. 2B, lanes 3 and 2). These concentrations were 4 to 5 times higher than the lowest active concentration of MBP-Oas1a tested. The results confirmed the previous finding of Kakuta et al. (2002) that Oas1a is an active 2-5A synthetase while Oas1btr is inactive. Oas1b was also shown to be inactive. However, an additional spot migrating above the free ATP but below the position of the oligoA dimer generated by Oas1a was observed only in the Oas1b reaction (Fig. 2B, compare lanes 2 and 3). This extra spot was only observed when poly(I:C) was included in the reaction mixture (Fig. 2C, compare lanes 2 and 3) suggesting that MBP-Oas1b, but not MBP-Oas1btr, is able to bind to and modify ATP after activation by dsRNA.

Poly(I:C)-binding activity of recombinant Oas1b proteins

The 2-5A synthetases require dsRNA to activate them to polymerize ATP into 2-5A (Wreschner et al., 1981). In a previous study, recombinant Oas1a and Oas1btr were shown to bind poly(I:C) efficiently (Kakuta, Shibata, and Iwakura, 2002). Oas1b poly(I:C) binding activity efficiency was tested by incubating bacterial lysates from cells expressing recombinant MBP-Oas1b with poly(I:C)-agarose. The bound proteins were separated by SDS-PAGE and detected by immunoblotting using anti-MBP antibody. Lysates from cells expressing MBP-Oas1a and MBP from the empty pMAL-C2g vector were used as positive and negative controls, respectively. Poly(I:C) bound efficiently to MBP-Oas1a and MBP-Oas1btr, consistent with previously published results (Kakuta, Shibata, and Iwakura, 2002), but less efficiently to MBP-Oas1b (Fig. 3). As expected, MBP did not bind to poly(I:C).

Analysis of the interaction of MBP-Oas1 proteins with WNV 3′ genomic RNA secondary structures

Single-stranded viral RNA genomes are predicted to have a significant amount of structure due to intramolecular RNA-RNA interactions and viral RNA stem-loop structures have been

shown to be able to activate 2′-5′ oligoadenylate synthetases (Desai et al., 1995; Maitra and Silverman, 1998; Sharp et al., 1999). Regions of the WNV-Eg101 genome RNA predicted to form long stem-loop structures by *mfold* analysis as well as by a whole genome fold (Palmenberg and Sgro, 1997) (Fig. 4A, D and H) were synthesized *in vitro* and used as probes in gel mobility shift assays with MBP-Oas1a, MBP-Oas1b, and MBP-Oas1btr. Increasing concentrations of each of the MBP-Oas1 proteins were tested with a constant amount of each probe. None of the Oas1 fusion proteins bound efficiently to Probe 1 (nts 10931-11029), the 3′ terminal stem-loop of the genome (Fig. 4A, B and C). Probe 2 (nts 10387-10448) was AU-rich and included the last 10 nts of the viral coding region, the viral stop codon, and the first 57 nts of the 3′ UTR. MBP-Oas1b bound to Probe 2 at concentrations between 10 ng to 200 ng (Fig. 4E), while MBP-Oas1a RNA binding to this probe was detected starting at 50 ng (Fig. 4F). MBP-Oas1btr did not bind to Probe 2 at any of the concentrations tested (Fig. 4G). Probe 3 (nts 10308-10364) was also AU-rich. Only MBP-Oas1b, at concentrations of 25 ng, 50 ng and 100 ng, exhibited detectable binding to Probe 3 (Fig. 4, I and J). The data indicate that full-length Oas1b and Oas1a, but not Oas1btr, can bind to partially dsRNAs. In contrast to its efficient binding to poly(I:C), Oas1btr did not bind to any of the viral RNAs tested.

Oas1b, but not Oas1btr, reduces Oas1a synthetase activity in vitro

A previous study reported that the inactive murine 2-5A synthetase, Oas1d, inhibited the *in vitro* synthetase activity of Oas1a in a dose-dependent manner (Yan et al., 2005). To investigate whether the inactive MBP-Oas1b or MBP-Oas1btr proteins could inhibit *in vitro* MBP-Oas1a synthetase activity, increasing molar ratios (0, 0.5X, 1X, 1.5X, and 2X) of these proteins were added to reactions containing a constant amount of MBP-Oas1a. MBP-Oas1b reduced MBP-Oas1a synthetase activity in a dose-dependent manner (Fig. 5A, lanes 2-6). In contrast, the addition of similar concentrations of MBP-Oas1btr caused no reduction in MBP-Oas1a synthetase activity (Fig. 5A, lanes 7-10). Both ATP and poly(I:C) were present in excess in these reactions.The data in Fig. 3 showed that the three Oas1 proteins studied bound poly(I:C) with different levels of efficiency: Oas1a ≥ Oas1btr > Oas1b. These data suggest that Oas1a would be expected to out-compete Oas1b for poly(I:C) binding. Also, if the inhibition were due solely to competition for poly(I:C), Oas1btr should also be expected to be able to inhibit Oas1a 2-5A synthesis. This was not observed to be the case. The results suggest that inhibition of Oas1a synthetase activity by Oas1b is mediated through protein-protein interactions and that Oas1b, but not Oas1btr, has a dominant negative effect on *in vitro* Oas1a synthetase activity.

Cells expressing Oas1b exhibit reduced 2-5A levels in response to poly(I:C) stimulation

The production of 2-5A *in vivo* in response to poly(I:C) stimulation was assessed in MEFs from transgenic C57BL/6 Oas1b knock-in mice (Oas1bKI) that express full-length Oas1b and control C57BL/6 mice that express Oas1btr (Scherbik et al., 2007). MEFs were incubated with 100 U/ml of Type I Universal IFN for 24 hrs to upregulate Oas1 expression and then transfected with 10 μg/ml poly(I:C) for 1 hr to induce 2-5A production. A FRET-assay that measures RNase L activity based on 2-5A levels was used to determine the amount of 2-5A produced *in vivo* (Thakur et al., 2005). Consistent with previously published reports (Andersen et al., 2007; Knight et al., 1980), low levels of 2-5A were observed in the untreated and IFN-treated MEFs. An increase in 2-5A levels was observed only in the C57BL/6 MEFs treated with IFN and poly(I:C) (Fig. 5B).

Due to the high homology between Oas1 proteins, antibodies cannot be used to distinguish individual Oas1 proteins by Western blotting. Oas1a and Oas1b mRNA levels in Oas1bKI and C57BL/6 MEFs were therefore assessed by real-time RT-PCR. IFN treatment resulted in about a 4-fold increase of Oas1a and Oas1b mRNA in Oas1bKI cells and a 2- to 3-fold

increase in C57BL/6 MEFs compared to the levels in control cells. Both Oas1a and Oas1b mRNA levels decreased after poly(I:C) transfection, possibly the result of RNase L-mediated degradation of mRNA, but the levels remained higher than in control cells indicating that Oas1 mRNA was upregulated by the IFN-treatment (Fig. 5C). Even though IFN-mediated Oas1 mRNA upregulation was less efficient in C57BL/6 MEFs compared to Oas1bKI MEFs, the levels of 2-5A production and RNase L activation were higher in C57BL/6 cells expressing Oas1btr. The results are consistent with the hypothesis that Oas1b has a dominant negative effect on Oas1a synthetase activity *in vivo*.

Discussion

The production of 2-5A and its subsequent activation of RNase L are important components of the IFN-induced antiviral response (Samuel, 2001). Of the eight mouse Oas1 genes, only Oas1a and Oas1g are active synthetases (Kakuta, Shibata, and Iwakura, 2002). The alleles of the Flv gene (Oas1b) determine whether mice produce a full-length or truncated Oas1b protein (Perelygin et al., 2002). Kakuta et al. (2002) reported that Oas1btr is an inactive synthetase and the current study showed that full-length Oas1b is also not capable of synthesizing 2-5A. Both Oas1b and Oas1btr, but none of the other inactive mouse Oas1 proteins, contain a 4 amino acid deletion in the P-loop that may prevent the folding of a catalytically functional structure as well as R90Q and R91Q substitutions in the ATP-substrate acceptor site and K195N, S203R and K209T substitutions in the ATP-substrate donor sites. The P-loop deletion as well as the substitutions in conserved residues characteristic of active synthetases are expected to be the reason for the lack of activity (Kakuta, Shibata, and Iwakura, 2002; Yamamoto, Sono, and Sokawa, 2000).

An intact P-loop motif was previously postulated to be required for ATP binding (Saraste, Sibbald, and Wittinghofer, 1990). Although both Oas1b and Oas1btr have the same 4 amino acid deletion in the 15 amino acid P-loop (VVMGGSSGKGt/aLKB, deleted residues are underlined and lower case letters indicate a sequence difference between Oas1a and Oas1b/btr, respectively), the data from *in vitro* 2-5A synthetase assays suggested that Oas1b but not Oas1btr could bind and modify ATP.

The Oas1btr and Oas1b proteins also differ in their RNA binding specificities. Oas1b bound to poly(I:C) less efficiently than did either Oas1a or Oas1btr. However, the interaction of Oas1b with poly(I:C) was of sufficient strength to activate it to bind and modify ATP. It was previously reported that the binding activities of RNAs do not correlate with their abilities to activate OAS proteins (Hartmann et al., 1998a). Oas1b bound to partially double-stranded viral stem-loop RNAs more efficiently than did Oas1a, while Oas1btr did not bind to any of the viral RNAs. The Oas1 dsRNA-binding domain(s) has not been identified but based on the crystal structure of porcine OAS, a protein that shares 56% identity with mouse Oas1b in residues important for folding, a bilobal conformation with the interface between the N- and C-terminal domains forming a 35Å long positively charged groove that could mediate interactions with RNA was predicted (Hartmann et al., 2003). Although enzymatic activity was completely abrogated by small C-terminal deletions of the human OAS1 protein, some dsRNA binding activity was retained by truncated proteins with more than half of the protein deleted, consistent with the existence of a large RNA activation site that spans both the catalytic and C-terminal OAS1 domains (Ghosh et al., 1991; Hartmann et al., 2003). Interestingly, viral stem loop RNA binding was observed only for the two full length Oas1 proteins tested suggesting that the C terminus is necessary for the binding of these RNAs. However, Oas1b bound to two of the three viral RNAs while Oas1a bound to only one of these RNAs suggesting the possibility of differential RNA recognition by different Oas1 proteins. A recent study identified the RNA consensus sequence NNWWNNNNNNNNNWGN as a recognition site for human OAS1 (Kodym, Kodym, and

Story, 2009). Although interaction between Oas1a and probe 2 was observed, no activation of Oas1a was observed after incubation of 1 μg of this protein with up to 50 μg/ml of probe 2 RNA; whereas, activation was observed with as little as 10 μg/ml poly(I:C) (data not shown). It was previously reported that activation of human 2-5A synthetase activity in HeLa cell extracts required considerably higher concentrations (360 nM) of HCV genomic RNA than of poly(I:C) (50 μg/ml) (Han and Barton, 2002).

In addition to its antiviral role, the OAS/RNase L pathway is involved in regulating mRNA turnover during cell differentiation, division and apoptosis (Ghosh et al., 2001; Kumar, Korutla, and Zhang, 1994; Salzberg et al., 1997). Because of the possibility that inappropriate or over production of 2-5A could cause significant damage, mechanisms to tightly regulate this pathway must exit in cells. Once 2-5A is synthesized, it is rapidly degraded by 2′- phosphodiesterase (Schmidt et al. 1978). However, the data from the present study and a previous study (Yan et al., 2005) indicate that multiple inactive murine Oas1 proteins can function as dominant negative inhibitors of active synthetases (Oas1a and Oas1g) and suggest that regulation also occurs at the level of 2-5A synthesis.

The expression of the Oas1a mRNA is detected in most tissues with the highest levels in digestive and lymphoid tissues (Kakuta, Shibata, and Iwakura, 2002; Salzberg et al., 1997; Shibata et al., 2001). The inactive Oas1d is exclusively expressed in ovaries. It was shown to inhibit the *in vitro* activity in a dose-dependent manner and was postulated to protect oocytes from a dsRNA-induced IFN response and cell death by reducing OAS/RNase L-mediated RNA degradation. Oas1c and Oas1e, which are also inactive synthetases, could partially compensate for this protective role in Oas1d-null mice (Yan et al., 2005) suggesting functional redundancy among the inactive synthetases. Oas1b mRNA is expressed at low levels in lung, uterus, and ovary and at higher levels in muscle tissue as well as lymphoid organs such as the thymus and spleen (Kakuta, Shibata, and Iwakura, 2002). Similar to Oas1d, full-length Oas1b, but not Oas1btr, inhibited *in vitro* Oas1a synthetase activity in a dose-dependent manner. Furthermore, 2-5A production in response to dsRNA stimulation in Oas1bKI cells, which express the full-length Oas1b, was markedly lower than in C57BL/6 cells, which express Oas1btr. These findings support a role for full-length Oas1b in the down-regulation of the Oas/RNase L pathway *in vivo*. Oas1b is expressed in a broad range of tissues suggesting that it is a major regulator of the Oas/RNase L pathway. However, other inactive Oas1 proteins must also be able to provide sufficient redundant function in mice expressing Oas1btr which is unable to function as a dominant negative inhibitor. It has been reported that tetramer formation is required for the activity of human OAS1 proteins and that tetramerization of the human OAS1 proteins is mediated through the CFK motif (Ghosh et al., 1997b). The active mouse synthetases Oas1a and Oas1g, have substitutions in the CFK motif as does Oas1d. However, Oas1b has an intact CFK motif and the gel mobility shift assay data (Fig. 4) suggest that Oas1b as well as Oas1a may form multimers (Fig. 4). Although it is not yet known whether tetramer formation is required for the synthetase activity of mouse Oas1 proteins, the dominant negative activity of inactive mouse Oas1 proteins strongly suggests that multimer formation is required for this inhibition.

Although Oas1b functions in the OAS/RNase L pathway to reduce the level of 2-5A produced, it is paradoxically not proviral because it also functions to specifically reduce the replication of flaviviruses by an alternative mechanism that is independent of RNase L (Sabin, 1952; Scherbik et al., 2006).

Materials and methods

Expression and purification of MBP-Oas1 Proteins

Murine Oas1a cDNA (accession No. X04958) and Oas1b cDNA (accession No. AF328926) were obtained as previously described (Perelygin et al., 2002). Oas1a and Oas1b plasmid DNAs were amplified with primers that added SnaBI and BamHI restriction sites to the PCR fragment and sub-cloned into the pMAL-c2G expression vector (New England Biolabs). The resulting constructs were designated pMAL-O1aQCR and pMAL-O1b. The pMAL-O1btr construct was generated using primers that introduced the premature codon into the Oas1b cDNA and also contained the SnaBI and BamHI restriction sites to clone the PCR fragment into pMAL-c2G.

Recombinant MBP-Oas1a protein was expressed in pMAL-O1aQCR transformed BL21 (non-D3E) cells grown in 250 mls of Rich Media containing 0.05% glucose and 75 μg/ml of carbenicillin (CRB). Expression was induced with 1 mM IPTG overnight at 16°C. Recombinant MBP-Oas1b protein was expressed in pMAL-O1b transformed BL21 (non-D3E) cells grown in 500 mls of TB Autoinduction media (Novagen) containing 0.05% glucose and 75 μg/ml of carbenicillin (CRB). Expression was auto-induced overnight at 16°C. Recombinant MBP-Oas1btr protein was expressed in pMAL-O1btr transformed BL21 (non-D3E) cells grown in 250 mls of Rich Media containing 0.05% glucose and 75 μg/ml of carbenicillin (CRB). Expression was induced with 0.5 mM IPTG overnight at 16°C.

Cells were pelleted by centrifugation at 5,000 × g for 15 min in a Avanti J30-I centrifuge using a JA-10 rotor (Beckman Coulter). The cells were resuspended in 5 ml of column buffer [20 mM tris-HCl, 200 mM NaCl, 1 mM EDTA, 10 mM β-ME and Complete Mini Protease inhibitor cocktail (Roche)] and frozen at −20°C until use.

Purification of MBP-Oas1 proteins

Recombinant Oas1 proteins were purified by affinity column purification using amylose resin. Bacterial cells were lysed with a SLM-Aminco French pressure cell (Heinemann) at 20,000 lb/in^2 and the lysate was centrifuged at 10,000 × g for 20 minutes. The soluble fraction was loaded onto an amylose resin column. The resin was washed with 100 ml of column buffer, and the MBP-fusion protein was then eluted from the column with 10 mM maltose in column buffer. MBP was cleaved from MBP-Oas1a using Genenase I (New England Biolabs) according to the manufacturer's protocol. The digestion mixture was loaded onto a hydroxyapatite column to remove maltose bound to MBP. Free MBP was then removed by passage through an amylose resin column. The flow-through containing Oas1a and trace amounts of the protease was collected, concentrated, and stored at −80°C until use. Pools of three or more partially purified recombinant Oas1 protein preparations were concentrated using a Microcon centrifugal filter device (50,000 nominal molecular weight limit) (Millipore) prior to use *in vitro* 2-5 A synthetase and EMSA experiments.

Western blotting

MBP-Oas1 proteins were separated by 10 % SDS-PAGE and transferred electrophoretically to a PVDF membrane, which was then blocked overnight at 4°C with 5 % BSA in TBS. The membrane was incubated at room temperature with a horseradish peroxidase (HRP) conjugated, monoclonal, murine anti-MBP (New England Biolabs) diluted 1:35,000 in a 5 % BSA-TBS solution at room temperature for 1.5 hrs. The membrane was washed with 0.05 % Tween-20-TBS solution (TBS-T). Alternatively, anti-OAS1 polyclonal antibody (Novus Biological) was diluted (1:1000) in a 5 % milk-TBS-T solution and incubated with the membrane overnight at 4°C. The membrane was washed with TBS-T and then incubated with anti-mouse IgG-HRP (Cell Signaling) diluted 1:2,000 in 5 % milk-TBS-t at room

temperature for 1 hr. The membrane was washed with TBS-T 3 times and once with TBS. Immunoreactive protein bands were detected by addition of West Pico Enhanced Chemiluminescence reagent (Pierce) and exposure to film.

Synthesis of RNA probes

Probe 1, Probe 2, and Probe 3 encompassed nts 10931-11029, 10387-10448, and 10308-10364 of the WNV Eg101 genome, respectively. RNA probes were synthesized using a MAXIscript *in vitro* transcription kit (Ambion) which utilizes a T7 RNA polymerase. Transcription reactions were carried out according to manufacturer′s protocol in the presence of ^{32}P-UTP (800 mCi/mol; Perkin-Elmer). Transcription products were separated by 6M urea PAGE. Gel slices containing RNA transcripts of the expected size were excised and the RNA was eluted from the gel slices by rocking overnight at 4°C in elution buffer (0.5 M NH_4OAC, 1 mM EDTA, and 0.2% SDS). The eluted RNA was filtered through a 0.45-μm cellulose acetate filter unit (Millipore) to remove gel pieces, precipitated with ethanol, resuspended in water, aliquoted, and stored at −80°C. The amount of radioactivity incorporated into each RNA probe was measured with a scintillation counter (model LS6500; Beckman).

Genome RNA fold

A secondary structure fold of the 11,029 nt WNV-Eg101 genomic RNA (accession no. AF260968) was generated by Ann Palmenberg using version 3.1 of MFOLD (Palmenberg and Sgro, 1997). In this fold, each base was algorithmically compared with all possible partners to determine the number of pairing partners within a free-energy range. The calculated pairing numbers (P-num values) provide a quantitative measure of the pairing probability for different partners in the context of multiple sub-optimal folds. Low P-num values (<3%) indicate high probability of pairing.

2-5 OAS activity assay

The reaction mixture (50 μl) contained 2′-5′ OAS activity assay buffer [20 mM HEPES-KOH pH 7.5, 50 mM KCl, 25 mM $Mg(OAC)_2$, 10 mM creatine phosphate, 1U/μl creatine kinase, 5 mM ATP, and 7 mM β-ME], 10 μCi α^{32}p-ATP and 50 ng/μl poly (I:C). MBP-Oas1 fusion proteins were added to reaction mixtures at increasing concentrations. Reactions were incubated at 30°C for 18 hrs and stopped by addition of 50 μl of Gel Loading Buffer II (95% formamide, 18 mM EDTA, 0.025% SDS, xylene cyanol, and bromophenol blue) (Ambion). Two to four μl of each reaction were loaded onto a 20% polyacrylamide gel and electrophoresed at 800 V for 3.5 hrs. Radiolabeled 2-5A was visualized by autoradiography.

Gel mobility shift assay

Reactions contained 1X Gel Shift Buffer (3% Ficoll-400, 20 mM sodium phosphate pH 7.2, 60 mM KCl, 1 mM $MgCl_2$, and 0.5 mM EDTA), 0.2 ul of RNasin, 50 ng of phenol-extracted yeast tRNA as a non-specific competitor, 10 mM (DTT) dithiothreitol, Oas1 protein and radiolabeled RNA probe. Reactions were incubated at room temperature for 20 minutes. An equal volume of gel-shift loading buffer (0.025% bromophenol blue, 0.025% xylene cyanol, 4% sucrose, and 1X TBE) was added and the reactions were electrophoresed on non-denaturing 5% polyacrylamide gels (39:1 acrylamide:bis-acrylamide and 1X TBE) at 120 V for 2 hrs at 4°C. The gel was dried and analyzed with a Fuji BAS 1800 analyzer (Fuji Photo Film Co.) and Image Gauge software (Science Lab, 98, version 3.12; Fuji Photo Film Co.).

Poly(I:C)-agarose binding assay

Recombinant MBP-Oas1a, MBP-Oas1b and MBP were expressed in BL21 STAR (DE3)pLysS bacterial cells grown in 35 mls of LB Media containing 0.05% glucose and 75 μg/ml of carbenicillin (CRB) at 37°C. At $O.D._{600}$ ~1.0, cultures were placed on ice for 10 minutes. Expression was induced with 1 mM IPTG for 15 minutes at 20°C. Cells were pelleted by centrifugation at 5,000 × g for 15 min in a Avanti J30-I centrifuge using a JA-10 rotor (Beckman Coulter). Cell pellets were resuspended in 1 ml of dsRNA-binding buffer [10 mM Hepes-KOH (pH 7.5), 3 mM $Mg(OAc)_2$, 0.3 mM EDTA, 50 mM KCl, 0.5 % glycerol] supplemented with protease Complete Mini EDTA-Free protease inhibitor cocktail (Roche). Cells were lysed by the addition of Cellytic cell lysis powder (Sigma-Aldrich) and incubation at 37°C for 15 minutes. Cell lysates were centrifuged at 15,000 × g for 12 minutes in a bench-top centrifuge (model 5415 D, Eppendorf). Clarified supernatant was added to 100 μl poly(I:C)-agarose bead slurry and rotated at room temperature for 2 hrs. Samples were then centrifuged at 700 × g for 5 minutes at 4°C and the supernatant containing the unbound protein fraction was collected. Samples were washed 5 times with 500 μl of dsRNA-binding buffer, centrifuged at 700 × g for 5 minutes at 4°C after each wash and the supernatant was discarded. The poly(I:C)-agarose bound to MBP-Oas1 proteins was resuspended in100 μl of dsRNA-binding buffer and 100 μl of 2X SDS sample buffer (125 mM Tris-HCl pH 6.8, 4 % SDS, 20 % Glycerol, 0.004 % bromophenol blue and 5 % 2-mercaptoethanol). Whole-cell lysate, unbound fraction and poly(I:C)-agarose bound fraction proteins were separated by 10 % SDS-PAGE and immunoblotted using HRP-conjugated anti-MBP antibody (New England Biolabs).

Cells

Single gene (Oas1b) knock in mice were generated as previously described (Scherbik et al., 2007). C57BL/6 and transgenic C57BL/6 Oas1b-KI MEF lines were SV-40 transformed and maintained as previously described (Scherbik et al., 2007).

FRET assay of RNase L activity for 2-5A levels

C57BL6 and Oas1b-KI MEFs were seeded into 6-well plates and grown overnight to about ~95% confluency. Cells were incubated with 100 U/ml type I universal IFN for 24 hrs. No IFN was added to the media for control cells. After 24 hrs, some of the IFN treated cells were transfected with 10 μg/ml poly(I:C) using Cellfectin (Invitrogen) for 1hr. Cells were than harvested and lysed by addition of NP-40 buffer [50 mM Tris-HCL (pH 7.2), 150 mM NaCl, 1% NP-40, 200 μM NaVO3, 2 mM EDTA, 5 mM MgCl2 and 5 mM DTT] that was pre-heated at 95°C for 3 minutes. The cell suspension was then heated to 95°C for 7 min. Cell debris was removed by centrifugation and the supernatant was applied to a Microcon centrifugal filter device (3,000 nominal molecular weight limit) (Millipore) and centrifuged for 45 minutes at 4°C. The volume was measured and the samples stored at −80°C until use.

RNase L activity was determined using a fluorescence resonance energy transfer (FRET) assay (Thakur et al., 2005). Recombinant human RNase L was produced in insect cells from a baculovirus vector and purified by FPLC (Townsend et al., 2008). The cleavable substrate consisted of a 36 nucleotide synthetic oligoribonucleotide [5′(6-FAM)-UUA UCA AAU UCU UAU UUG CCC CAU UUU UUU GGU UUA- BHQ-1)-3′] derived from respiratory syncytial virus (Thakur et al., 2005). The RNA sequence contains several cleavage sites for RNase L (UU or UA). Triplicate 5μl aliquots of 1:10 dilution of each sample in DEPC treated water were added to 96-well black polystyrene microtiter plates (Corning) on ice. The reactions (45μl) contained 100 nM FRET probe, 25 nM RNase L, 25 mM Tris–HCl (pH 7.4), 100 mM KCl, 10 mM $MgCl_2$, 100 μM ATP, and 7.2 mM 2-mercaptoethanol. RNase L was the last component added. The plates were incubated at 20°C protected from light. To generate a standard curve, authentic trimeric 2-5A (>95% purity) diluted to final

concentrations of 0.05 0.1, 0.3, 1, 3, 10, and 30 nM in DEPC-treated water was used. Fluorescence was measured at 5, 30, and 60, min with a Wallac 1420 fluorimeter (Perkin-Elmer LAS Inc., USA) (excitation 485 nm/emission 535 nm with a 0.1s integration time).

Real-time qRT-PCR

Real-time quantitative reverse transcription-PCR (qRT-PCR) analysis of mouse Oas1a and Oas1b mRNAs was performed with Assays-on-Demand 20x primer and fluorogenic TaqMan FAM/TAMRA (6-carboxyfluorescein/6-carboxytetramethylrhodamine)-labeled hybridization probe mixes (Applied Biosystems). Glyceraldehyde-3-phosphate dehydrogenase (GAPDH) mRNA was used as an endogenous control and was detected using TaqMan mouse GAPDH Control Reagents primers and probe (Applied Biosystems). One-step RT-PCR was performed for each target gene and for the endogenous control in a singleplex format using 200 ng of RNA and the TaqMan one-step RT-PCR master mix reagent kit (Applied Biosystems). The cycling parameters were as follows: reverse transcription at 48°C for 30 min, AmpliTaq activation at 95°C for 10 min, denaturation at 95°C for 15 s, and annealing/extension at 60°C for 1 min (cycle repeated 40 times). Triplicate C_t values were analyzed with the comparative $C_t(\Delta\Delta C_t)$ method (Applied Biosystems) using Microsoft Excel software. The amount of target ($2^{-\Delta\Delta Ct}$) was determined by normalization to endogenous control (GAPDH) and relative to a cell-type specific untreated calibrator sample.

Acknowledgments

This work was supported in part by Public Health Service research grants AI045135 and AI048088 to M.A.B. from the National Institute of Allergy and Infectious Diseases, National Institutes of Health and CA044059 to R.H.S. from the National Cancer Institute, National Institutes of Health. We thank Ann C. Palmenberg for providing the WNV genome RNA fold data, Andrey A. Perelygin for providing the initial clones of the mouse Oas1 cDNAs and William G. Davis and Mohamed Emara for technical advise.

References

Andersen JB, Li XL, Judge CS, Zhou A, Jha BK, Shelby S, Zhou L, Silverman RH, Hassel BA. Role of 2-5A-dependent RNase-L in senescence and longevity. Oncogene. 2007; 26(21):3081–8. [PubMed: 17130839]

Benech P, Mory Y, Revel M, Chebath J. Structure of two forms of the interferon-induced (2′-5′) oligo A synthetase of human cells based on cDNAs and gene sequences. Embo J. 1985; 4(9):2249–56. [PubMed: 2416561]

Brinton MA. The molecular biology of West Nile Virus: a new invader of the western hemisphere. Annu Rev Microbiol. 2002; 56:371–402. [PubMed: 12142476]

Desai SY, Patel RC, Sen GC, Malhotra P, Ghadge GD, Thimmapaya B. Activation of interferon-inducible 2′-5′ oligoadenylate synthetase by adenoviral VAI RNA. J Biol Chem. 1995; 270(7): 3454–61. [PubMed: 7531709]

Floyd-Smith G, Slattery E, Lengyel P. Interferon action: RNA cleavage pattern of a (2′-5′)oligoadenylate--dependent endonuclease. Science. 1981; 212(4498):1030–2. [PubMed: 6165080]

Ghosh A, Desai SY, Sarkar SN, Ramaraj P, Ghosh SK, Bandyopadhyay S, Sen GC. Effects of mutating specific residues present near the amino terminus of 2′-5′-oligoadenylate synthetase. J Biol Chem. 1997a; 272(24):15452–8. [PubMed: 9182577]

Ghosh A, Sarkar SN, Guo W, Bandyopadhyay S, Sen GC. Enzymatic activity of 2′-5′-oligoadenylate synthetase is impaired by specific mutations that affect oligomerization of the protein. J Biol Chem. 1997b; 272(52):33220–6. [PubMed: 9407111]

Ghosh A, Sarkar SN, Rowe TM, Sen GC. A specific isozyme of 2′-5′ oligoadenylate synthetase is a dual function proapoptotic protein of the Bcl-2 family. J Biol Chem. 2001; 276(27):25447–55. [PubMed: 11323417]

Ghosh SK, Kusari J, Bandyopadhyay SK, Samanta H, Kumar R, Sen GC. Cloning, sequencing, and expression of two murine 2′-5′-oligoadenylate synthetases. Structure-function relationships. J Biol Chem. 1991; 266(23):15293–9. [PubMed: 1651324]

Han JQ, Barton DJ. Activation and evasion of the antiviral 2′-5′ oligoadenylate synthetase/ribonuclease L pathway by hepatitis C virus mRNA. RNA. 2002; 8(4):512–25. [PubMed: 11991644]

Hartmann R, Justesen J, Sarkar SN, Sen GC, Yee VC. Crystal structure of the 2′-specific and double-stranded RNA-activated interferon-induced antiviral protein 2′-5′-oligoadenylate synthetase. Mol Cell. 2003; 12(5):1173–85. [PubMed: 14636576]

Hartmann R, Norby PL, Martensen PM, Jorgensen P, James MC, Jacobsen C, Moestrup SK, Clemens MJ, Justesen J. Activation of 2′-5′ oligoadenylate synthetase by single-stranded and double-stranded RNA aptamers. J Biol Chem. 1998a; 273(6):3236–46. [PubMed: 9452437]

Hartmann R, Olsen HS, Widder S, Jorgensen R, Justesen J. p59OASL, a 2′-5′ oligoadenylate synthetase like protein: a novel human gene related to the 2′-5′ oligoadenylate synthetase family. Nucleic Acids Res. 1998b; 26(18):4121–8. [PubMed: 9722630]

Kakuta S, Shibata S, Iwakura Y. Genomic structure of the mouse 2′,5′-oligoadenylate synthetase gene family. J Interferon Cytokine Res. 2002; 22(9):981–93. [PubMed: 12396720]

Kerr IM, Brown RE. pppA2′p5′A2′p5′A: an inhibitor of protein synthesis synthesized with an enzyme fraction from interferon-treated cells. Proc Natl Acad Sci U S A. 1978; 75(1):256–60. [PubMed: 272640]

Knight M, Cayley PJ, Silverman RH, Wreschner DH, Gilbert CS, Brown RE, Kerr IM. Radioimmune, radiobinding and HPLC analysis of 2-5A and related oligonucleotides from intact cells. Nature. 1980; 288(5787):189–92. [PubMed: 6159552]

Kodym R, Kodym E, Story MD. 2′-5′-Oligoadenylate synthetase is activated by a specific RNA sequence motif. Biochem Biophys Res Commun. 2009; 388(2):317–22. [PubMed: 19665006]

Kumar R, Korutla L, Zhang K. Cell cycle-dependent modulation of alpha-interferon-inducible gene expression and activation of signaling components in Daudi cells. J Biol Chem. 1994; 269(41):25437–41. [PubMed: 7929242]

Maitra RK, Silverman RH. Regulation of human immunodeficiency virus replication by 2′,5′-oligoadenylate-dependent RNase L. J Virol. 1998; 72(2):1146–52. [PubMed: 9445011]

Mashimo T, Lucas M, Simon-Chazottes D, Frenkiel MP, Montagutelli X, Ceccaldi PE, Deubel V, Guenet JL, Despres P. A nonsense mutation in the gene encoding 2′-5′-oligoadenylate synthetase/L1 isoform is associated with West Nile virus susceptibility in laboratory mice. Proc Natl Acad Sci U S A. 2002; 99(17):11311–6. [PubMed: 12186974]

Palmenberg AC, Sgro JY. Topological organization of picornaviral genomes: Statistical Prediction of RNA structural signals. Seminars in VIROLOGY. 1997; 8(3):231–241.

Perelygin AA, Scherbik SV, Zhulin IB, Stockman BM, Li Y, Brinton MA. Positional cloning of the murine flavivirus resistance gene. Proc Natl Acad Sci U S A. 2002; 99(14):9322–7. [PubMed: 12080145]

Rebouillat D, Marie I, Hovanessian AG. Molecular cloning and characterization of two related and interferon-induced 56-kDa and 30-kDa proteins highly similar to 2′-5′ oligoadenylate synthetase. Eur J Biochem. 1998; 257(2):319–30. [PubMed: 9826176]

Sabin AB. Nature of Inherited Resistance to Viruses Affecting the Nervous System. Proc Natl Acad Sci U S A. 1952; 38(6):540–6. [PubMed: 16589143]

Salzberg S, Hyman T, Turm H, Kinar Y, Schwartz Y, Nir U, Lejbkowicz F, Huberman E. Ectopic expression of 2-5A synthetase in myeloid cells induces growth arrest and facilitates the appearance of a myeloid differentiation marker. Cancer Res. 1997; 57(13):2732–40. [PubMed: 9205084]

Samuel CE. Antiviral actions of interferons. Clin Microbiol Rev. 2001; 14(4):778–809. table of contents. [PubMed: 11585785]

Saraste M, Sibbald PR, Wittinghofer A. The P-loop--a common motif in ATP- and GTP-binding proteins. Trends Biochem Sci. 1990; 15(11):430–4. [PubMed: 2126155]

Scherbik SV, Kluetzman K, Perelygin AA, Brinton MA. Knock-in of the Oas1b(r) allele into a flavivirus-induced disease susceptible mouse generates the resistant phenotype. Virology. 2007; 368(2):232–7. [PubMed: 17904183]

Scherbik SV, Paranjape JM, Stockman BM, Silverman RH, Brinton MA. RNase L plays a role in the antiviral response to West Nile virus. J Virol. 2006; 80(6):2987–99. [PubMed: 16501108]

Scherbik SV, Stockman BM, Brinton MA. Differential expression of interferon (IFN) regulatory factors and IFN-stimulated genes at early times after West Nile virus infection of mouse embryo fibroblasts. J Virol. 2007; 81(21):12005–18. [PubMed: 17804507]

Sharp TV, Raine DA, Gewert DR, Joshi B, Jagus R, Clemens MJ. Activation of the interferon-inducible (2′-5′) oligoadenylate synthetase by the Epstein-Barr virus RNA, EBER-1. Virology. 1999; 257(2):303–13. [PubMed: 10329541]

Shibata S, Kakuta S, Hamada K, Sokawa Y, Iwakura Y. Cloning of a novel 2′,5′-oligoadenylate synthetase-like molecule, Oasl5 in mice. Gene. 2001; 271(2):261–71. [PubMed: 11418248]

Thakur CS, Xu Z, Wang Z, Novince Z, Silverman RH. A convenient and sensitive fluorescence resonance energy transfer assay for RNase L and 2′,5′ oligoadenylates. Methods Mol Med. 2005; 116:103–13. [PubMed: 16000857]

Townsend HL, Jha BK, Han JQ, Maluf NK, Silverman RH, Barton DJ. A viral RNA competitively inhibits the antiviral endoribonuclease domain of RNase L. RNA. 2008; 14(6):1026–36. [PubMed: 18426919]

Wreschner DH, McCauley JW, Skehel JJ, Kerr IM. Interferon action--sequence specificity of the ppp(A2′p)nA-dependent ribonuclease. Nature. 1981; 289(5796):414–7. [PubMed: 6162102]

Yamamoto Y, Sono D, Sokawa Y. Effects of specific mutations in active site motifs of 2′,5′-oligoadenylate synthetase on enzymatic activity. J Interferon Cytokine Res. 2000; 20(3):337–44. [PubMed: 10762083]

Yan W, Ma L, Stein P, Pangas SA, Burns KH, Bai Y, Schultz RM, Matzuk MM. Mice deficient in oocyte-specific oligoadenylate synthetase-like protein OAS1D display reduced fertility. Mol Cell Biol. 2005; 25(11):4615–24. [PubMed: 15899864]

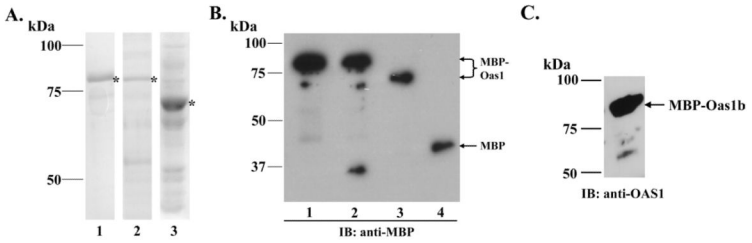

Figure 1. Expression and purification of recombinant MBP-Oas1 proteins

(A) MBP-Oas1 proteins were expressed in bacteria, partially purified on amylose columns, separated by 10% SDS-PAGE and visualized by Coomassie blue staining. Lane 1, MBP-Oas1a. Lane 2, MBP-Oas1b. Lane 3, MBP-Oas1btr. Asterisks indicate the positions of the MBP-Oas1 fusion proteins. (B) Immunoblot of partially purified MBP-Oas1 proteins detected with anti-MBP-HRP antibody. Lane 1, MBP-Oas1a. Lane 2, MBP-Oas1b. Lane 3, MBP-Oas1btr. Lane 4, MBP. (C) Immunoblot of partially purified MBP-Oas1b protein detected with anti-OAS1 antibody.

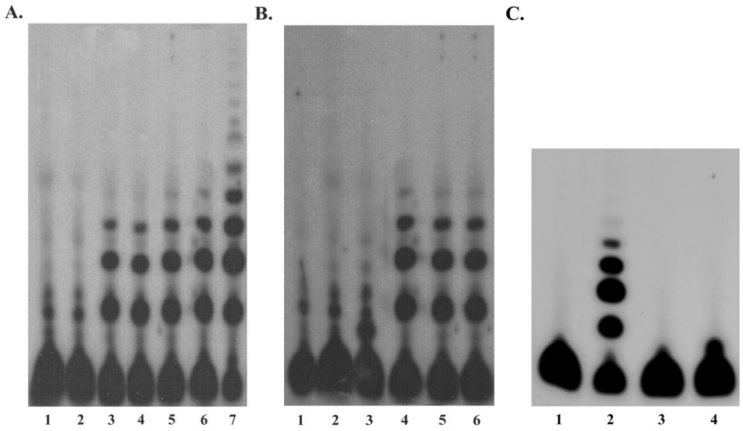

Figure 2. Analysis of MBP-Oas1 protein 2-5A synthetase activity

Different amounts of MBP-Oas1 proteins were incubated with α^{32}p-ATP and poly (I:C) for 18 hrs at 30°C. Four μl (A) or two μl (B and C) of each reaction were then electrophoresed on a 20% polyacrylamide urea denaturing gel. (A) Analysis of MBP-Oas1a 2-5A synthetase activity. Reactions contained: Lane 1, No protein. Lane 2, 16 μg of MBP. Lane 3, 0.75 μg of Oas1a. Lanes 4-7, 0.5 μg, 0.75 μg, 1 μg, and 16 μg of MBP-Oas1a, respectively. (B) Analysis of MBP-Oas1b 2′-5′ Oas activity. Reactions contained: Lane 1, No protein. Lane 2, 2.3 μg of MBP-Oas1btr. Lane 3, 2.6 μg of MBP-Oas1b. Lanes 4-6, 1 μg, 0.75 μg, and 0.5 μg of MBP-Oas1a, respectively. (C) Analysis of the effect of poly(I:C) on MBP-Oas1b synthetase activity. Reactions contained: Lane 1, No protein. Lane 2, 1.5 μg of MBP-Oas1b without poly(I:C). Lane 3, 1.5 μg of MBP-Oas1b with 50 μg/ml poly(I:C). Lane 4, 0.5 μg of MBP-Oas1a with poly(I:C). The data shown are representative of results obtained from at least three repeats using different pooled protein preparations.

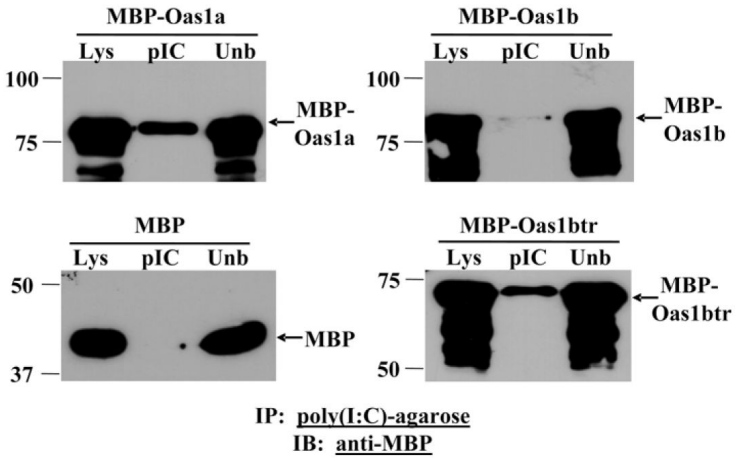

Figure 3. Analysis of Oas1 protein dsRNA binding activity

The ability of MBP-Oas1a, MBP-Oas1b or MBP to bind dsRNA poly(I:C)-agarose was tested. Bound RNA-protein complexes were separated by 10% SDS-PAGE. Immunoblotting was performed using anti-MBP antibody. Lys, lysate; pIC, poly(I:C)-bound fraction; Unb, unbound fraction. The data shown are representative of results obtained from at least three repeats.

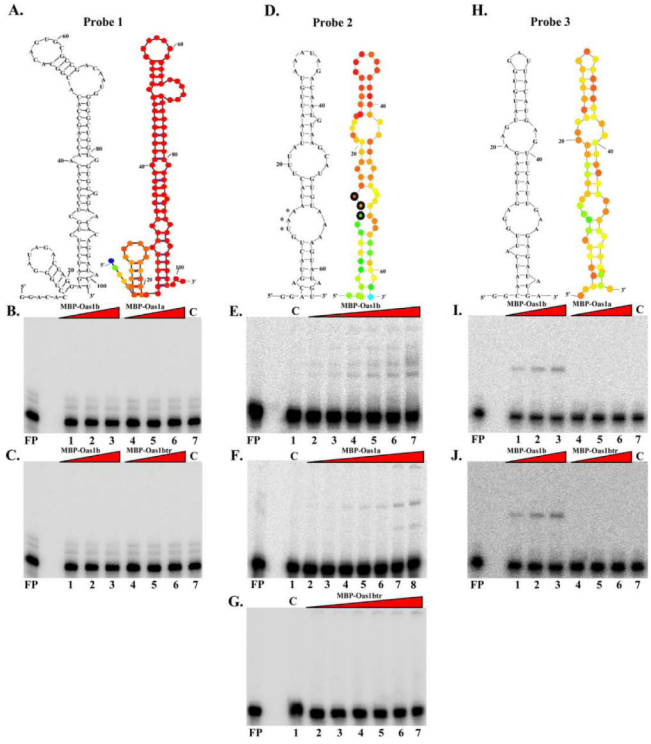

Figure 4. Analysis of Oas1 protein binding activity for partially dsRNA probes

(A, D, and H) WNV Eg101 genome RNA structures predicted by MFOLD version 3.1 (black) of just the stem loop sequences and by a whole genome fold (color). The nts with the highest probability of pairing (<3%) are indicated in red, with orange next, then yellow, and then green. Probe 1 (A), Probe 2 (D), and Probe 3 (H) RNAs were radiolabeled by incorporation of ^{32}p-UTP during *in vitro* transcription. Gel mobility shift assays with Probe 1 (1,000 cpm). (B) Lanes 1-3, MBP-Oas1b at 25, 50 and 100 ng. Lanes 4-6, MBP-Oas1a at 25, 50 and 100 ng. Lane 7, 100 ng of MBP. (C) Lanes 1-3, MBP-Oas1b at 25, 50 and 100 ng. Lanes 4-6, MBP-Oas1btr at 25, 50 and 100 ng. Lane 7, 100 ng of MBP. Gel mobility shift assays with Probe 2 (2,000 cpm). (E) Lane 1, 200 ng of MBP. Lanes 2-7, MBP-Oas1b at 10, 25, 50, 75, 100, and 200 ng. (F) Lane 1, 400 ng of MBP. Lanes 2-7, MBP-Oas1a at 10, 25, 50, 75, 100, 200, and 400 ng. (G) Lane 1, 200 ng of MBP. Lanes 2-7, MBP-Oas1btr at 10, 25, 50, 75, 100, and 200 ng. Gel mobility shift assays with Probe 3 (1,000 cpm). (I) Lanes 1-3, MBP-Oas1b at 25, 50 and 100 ng. Lanes 4-6, MBP-Oas1a at 25, 50 and 100 ng. Lane 8, 100 ng of MBP. (J) Lanes 1-3, MBP-Oas1b at 25, 50 and 100 ng. Lanes 4-6, MBP-Oas1a at 25, 50 and 100 ng. Lane 8, 100 ng of MBP. Components of binding reactions were separated on a 6 % polyacrylamide non-denaturing gel. Bands on the dried gel were detected using a Bio-Image Analyzer PhosphorImager (Molecular Dynamics). FP, free probe. The data shown are representative of results obtained from at least three repeats using different pooled protein preparations.

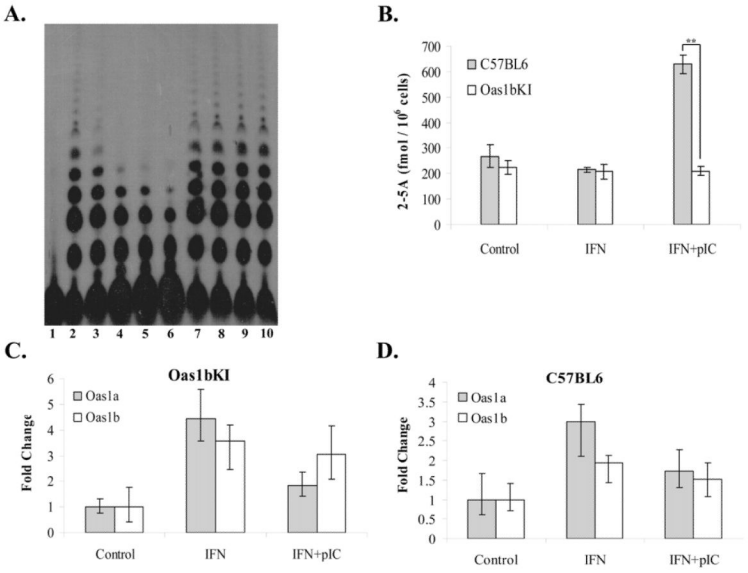

Figure 5. Oas1b reduces 2-5A production *in vitro* and *in vivo*

(A) *In vitro* 2-5A production. All reactions contained α^{32}p-ATP, poly (I:C), and 1 μg of MBP-Oas1a. Lane 1, no additional protein. Lanes 2-6, MBP-Oas1a and 0, 0.5X, 1X, 1.5X, or 2X of MBP-Oas1b, respectively. Lanes 7-10, MBP-Oas1a and 0, 0.5X, 1X, 1.5X, or 2X of MBP-Oas1btr, respectively. The products of each reaction were separated on a 20% polyacrylamide-urea denaturing gel. The data shown are representative of results obtained from at least three repeats using different pooled protein preparations. (B) Levels of 2-5A in C57BL6 and Oas1b-KI cells. MEFs were seeded into 6-well plates and grown overnight to about ~100% confluency and then incubated with 100 U/ml type I universal IFN for 24 hrs (IFN). No IFN was added to the media of the control cells. After 24 hrs, some wells of IFN treated cells were transfected with 10 μg/ml poly(I:C) for 1hr (IFN +pIC). The amounts of 2-5A in cell extracts were measured using a FRET assay of RNase L activity. Data are expressed as amount of 2-5A per 10^6 cells. The values are averages of three replicate samples each assayed in triplicate. The standard error (SE) of the mean is indicated. The results shown are representative of three experiments each done in triplicate. The data were subjected to *Student's t-test* statistical analysis done with EXCEL software. ** denotes $p = 0.0133$. (C and D) Analysis of changes in the expression levels of the Oas1a and Oas1b genes in Oas1bKI and C57BL6 cells after IFN treatment or IFN and poly(IC) treatment by qRT-PCR. The relative fold change in expression compared to the level of the same mRNA present in cell-type specific untreated controls is expressed in RQ units. Error bars represent the SE ($n = 3$) and are based on an $RQ_{Min/Max}$ of the 95% confidence level.